Model For Rainfall Excess Patterns on Randomly Heterogeneous Areas

By R. E. Smith[1] and D. C. Goodrich,[2] Members, ASCE

Abstract: A model is presented that can simulate infiltration from rainstorms on areas exhibiting random variation in saturated hydraulic conductivity K_S. Heterogeneity in the capillary drive (or length scale) parameter G can be treated as well. The method is based on a point infiltration model that includes the Green-Ampt or Smith-Parlange infiltration functions. The runoff area is characterized as an ensemble of infiltrating points or flow path strips that provides runoff to a receiving channel. The model is developed by simulation of a large ensemble using Latin hypercube sampling. The infiltration expression is responsive to a changing rainfall rate r and is easily characterized using the basic infiltration parameters K_S and G, plus a third parameter based only on the coefficient of variation of K_S or G. Areal heterogeneity causes a rainfall-dependent change in the areal effective value for K_S, called $K_e(r)$. The infiltration expression contains rainfall rate as a variable, and observed storms with temporal rainfall patterns may easily be treated. Moreover, the new expression eliminates the explicit concept of ponding time as a separate calculation. The effect of heterogeneous infiltration parameters is demonstrated using several field cases.

INTRODUCTION

There is general acknowledgment of the important challenge in hydrology to make physical process-based models applicable at larger than plot scales. This is often termed upscaling. It is both difficult and costly to sample an area thoroughly enough to know what the areal average of a measurable parameter may be. Also, it is usually misleading and inaccurate to assume that average parameter values may be used for heterogeneous areas, because the processes underlying those parameters are often highly nonlinear and an average parameter in a nonlinear function does not behave as does an ensemble of nonlinear processes. Thus seeking an areal effective value by fitting a nonlinear infiltration model to large-area data such as stream runoff is likely to produce misleading results. Perhaps the most comprehensive recent discussion of the challenges involved in upscaling physically based models was that of Grayson et al. (1992), in which the very idea of using physically based models at a watershed scale was called into question. Infiltration of rainwater into the soil is one of the processes known to exhibit significant random spatial variation (Nielsen et al. 1973; Sharma et al. 1980; Hjelmfelt and Burwell 1984).

The soil hydraulic parameter of principle interest in most studies has been saturated hydraulic conductivity K_S. The measurements of K_S have so consistently shown a lognormal random variation [Nielsen et al. (1973) and Vieira et al. (1981), for example] that $\log(K_S)$ is now commonly assumed as the random variable in theoretical studies [Yeh et al. (1985), for example]. The simulation studies of Bresler and Dagan (1983) and Chen et al. (1994) treated lognormal variation in K_S within the context of a Green-Ampt infiltration model, but in both cases the distribution properties of the wetting front and the determination of an ensemble mean the wetting front was the focus. In contrast, the role of heterogeneous soil properties in ensemble infiltration rates is the focus of these studies.

Studies of runoff from surfaces with heterogeneous saturated hydraulic conductivity have shown the general effect of both random and deterministic variation in K_S (Smith and Hebbert 1979; Goodrich et al. 1988; Woolhiser et al. 1996). Random variations in K_S have greater influence on runoff for lower rates of rainfall r, where runoff may be significant but is a small fraction of the total rainfall depth R. For very high rates of rainfall, infiltration rates and thus their variations have much less importance. Hawkins and Cundy (1987) showed that there is a relation between rainfall rate and the areal effective steady infiltration rate for heterogeneous areas. That relation is one of the interactions between intensity and the distributed infiltration rate, which are quantified below.

The method used in this study is to simulate the net infiltration behavior of an area characterized by lognormally distributed values of soil infiltration parameters and to represent the ensemble behavior by an expression that is simple to apply. Maller and Sharma (1981) performed a simulation of ensemble infiltration for steady rainfall rates, and obtained results for infiltration on a heterogeneous area, assuming a time explicit point infiltration relation based on the Philip two-parameter relation. Their method was to numerically integrate complex probability expressions for ponding time and for subsequent infiltration, but they reported no relation that could be applied for practical hydrological purposes. Sivapalan and Wood (1986) started also with the two-term Philip expression for point infiltration and made some significant approximations to derive an expression for areal mean rates, but these expressions were also mathematically formidable, involving error function evaluations. Their method also assumed a uniform rainfall rate, and they made no validation of their approximations. Woolhiser and Goodrich (1988) and Smith et al. (1990) represented distributed K_S values using stratified sampling from the lognormal distribution (as described in more detail below) and applied these values to equal area strips of a catchment surface. This method, schematically illustrated in Fig. 1, simulates cross-slope variability in K_S and is suitable for variable rainfall intensities but requires all infiltration and routing computations to be repeated for each strip, which substantially increases computation. Nachabe et al. (1997) and Woolhiser et al. (1996) studied a few special cases of variation along a flow path, which would lend insight into higher order heterogeneity assumptions.

Here, one assumes random variation of the infiltration behavior sampled for noninteractive points or similar flow path strips, but one seeks an expression for the areal mean infiltration on such a heterogeneous runoff surface. The expression should be applicable to storms of variable intensity patterns, be computationally relatively simple, and match ensemble simulation results very closely. The use of a simulation in this

[1]Res. Hydr. Engr., Agricultural Research Service-U.S. Dept. of Agr., Engrg. Res. Ctr., Colorado State Univ., Fort Collins, CO 80523.

[2]Res. Hydr. Engr., Agricultural Research Service-U.S. Dept. of Agr., Southwest Watershed Res. Ctr., Tucson, AZ 85719.

Note. Discussion open until March 1, 2001. To extend the closing date one month, a written request must be filed with the ASCE Manager of Journals. The manuscript for this paper was submitted for review and possible publication on April 20, 1998. This paper is part of the ***Journal of Hydrologic Engineering***, Vol. 5, No. 4, October, 2000. ©ASCE, ISSN 1084-0699/00/0004-0355–0362/$8.00 + $.50 per page. Paper No. 18146.

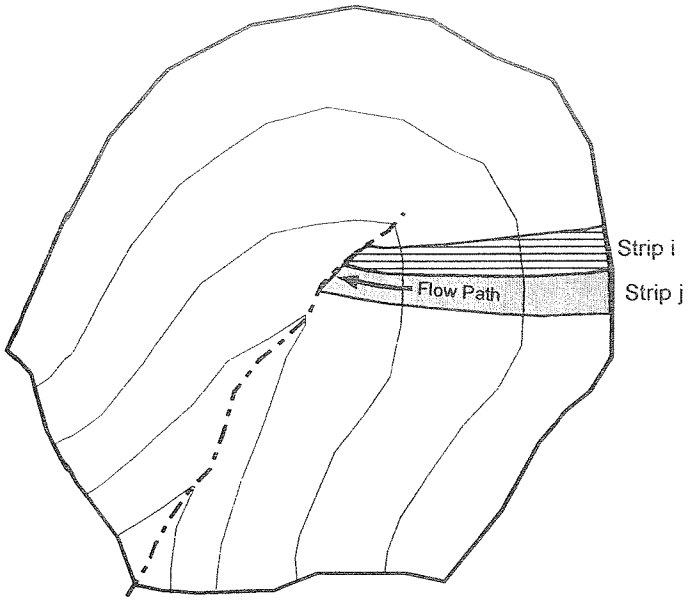

FIG. 1. Runoff Area of Interest Is Divided into Pieces along Flow Lines for Characterizing Random Spatial Variation, as in Woolhiser and Goodrich (1988)

case is most appropriate because it represents theoretical (numerical) experiments that cannot be done practically with a physical experiment. Although the heterogeneous infiltration relation incorporates a particular mathematical description of point infiltration, it is not dependent upon it. In the final section one considers evidence for the validity of an ensemble or field-scale infiltration relationship and applies the method to several cases.

POINT INFILTRATION MODEL

A robust analytically derived infiltration model is used to represent soil infiltration behavior at any point on an area of interest. Effective saturated hydraulic conductivity K_S is one of two physically related parameters for point infiltration functions, and the second is the intrinsic capillary drive of the soil G, also called the capillary length scale (White and Sully 1987). The value G can be related to the soil sorptivity S (Philip 1957) or computed from the soil unsaturated hydraulic conductivity characteristic $K(h)$

$$G = \frac{S^2}{2K_S\Delta\theta_i} \cong \frac{1}{K_S}\int_{-\infty}^{0} K(h)\, dh \tag{1}$$

where $\Delta\theta_i$ represents the soil initial condition is the initial saturation deficit, $\theta_S - \theta_i$; and θ_S = saturated water content. The value G can be thought of as the K-weighted mean capillary potential of the soil and plays an important role in various quasi-linear analyses of unsaturated flow (Philip 1985).

A simplified description of infiltration functions can be obtained if scaled values are used. To this end one may define the following dimensionless variables:

$$r_* = \frac{r}{K_S};\quad f_* = \frac{f}{K_S} \tag{2a,b}$$

$$I_* = \frac{I}{G\Delta\theta_i};\quad t_* = \frac{tK_S}{G\Delta\theta_i} \tag{2c,d}$$

where the variable I represents the cumulative depth of infiltration $\int f\, dt$.

The model used here is the three-parameter model of Parlange et al. (1982), which can represent either a Green and Ampt (1911) or a Smith and Parlange (1978) soil, or any behavior in between. It describes the infiltrability of a soil either in terms of time during a steady rain or in terms of I for a rain of variable intensity $r(t)$. The function may be expressed as follows (Smith et al. 1993):

$$f_{c^*} = \left[1 + \frac{\alpha}{\exp[\alpha I_*] - 1}\right] \tag{3}$$

in which f_{c^*} = scaled soil infiltration capacity rate, or infiltrability; and α = parameter, from 0 to 1, designating soil behavior.

When α is 1, (3) becomes the Smith-Parlange equation:

$$f_{c^*} = [1 - \exp(-I_*)]^{-1} \tag{4}$$

and when α approaches 0, (3) asymptotically approaches the Green-Ampt expression:

$$f_{c^*} = \left[\frac{I_* + 1}{I_*}\right] \tag{5}$$

At small values of I_* or at small times, either expression approaches the fundamental gravity-free or horizontal infiltration expression:

$$f_{c^*} = \frac{1}{I_*} \tag{6}$$

The actual infiltration rate during a storm f is the smaller of f_c or intensity r.

Relationships between time and I or f may be found from (3) [and (2)] by substituting either $f = dI/dt$ or $I = \int f\, dt$ and solving (Smith et al. 1993). In the latter case, one obtains, in terms of the dimensionless variables

$$(t_* - t_{p^*})(1 - \alpha) = \frac{1}{\alpha}\ln\left[\frac{(f_* - 1 + \alpha)(r_{p^*} - 1)}{(r_{p^*} - 1 + \alpha)(f_* - 1)}\right] - \ln\left[\frac{f_*(r_{p^*} - 1)}{r_{p^*}(f_* - 1)}\right],\quad t_* > t_{p^*} \tag{7}$$

in which subscript p refers to ponding when (3) is satisfied by $f_c = r$.

ASSUMPTIONS AND METHODS

Sampling

A runoff area of a single soil type possessing random heterogeneity in soil properties and composed of a number (ensemble) of runoff paths to the outlet is assumed. Each runoff path to the outlet is a single sample, the sum of which constitutes the total runoff area, as in Fig. 1. The arguments made here would equally apply to an area in which runoff was ignored and was assumed composed of an ensemble of representative points, each point representing one realization from the distribution of properties describing the random variation of the soil.

The ensemble behavior is simulated using a numerical method known as Latin hypercube (LH) sampling (McKay et al. 1979), referred to subsequently as the LH method. This method should be distinguished from Monte Carlo sampling, which is a statistical method requiring a very large number of random samples to obtain an accurate representation of the underlying distribution for a parameter within a system. The LH sampling is a numerical method and can more efficiently simulate the effect of random variation of one or a number of parameters. Fig. 2 illustrates the numerical representation of a parameter from an arbitrary distribution. The probability density function (PDF) is divided into n equal subareas, equivalent

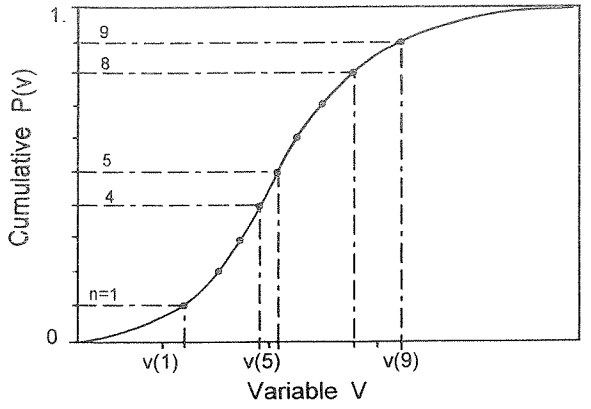

FIG. 2. Arbitrary CDF Curve Illustrates Principle of LH Sampling; Cumulative Probability Axis Is Divided into *n* Equal Segments that Delineate Corresponding Portions of Range of Variable *v* To Be Represented in Equal Probability Sampling

to dividing the ordinate of the cumulative distribution function (CDF) into n equal parts. The first moment of each of the n subareas is used to represent that subarea of the PDF in a set of n simulations of a system, the mean response of which represents the net effect of the distributed variate within its system. In Fig. 2, n is 10 and three of the subarea segments are illustrated.

To obtain a physically meaningful areal mean relation, one uses (7) to relate areal mean $f = f_e$ to areal mean $I = I_e$ at each t through a storm. These are defined as areal expected values for spatially heterogeneous values of parameters in (3) over an ensemble of n points

$$f_e(t) = \frac{1}{n}\sum_{i=1}^{n} f(t, K_{S,i}, G_i) \tag{8a}$$

$$I_e(t) = \frac{1}{n}\sum_{i=1}^{n} \int_0^t f(t, K_{S,i}, G_i)\, dt \tag{8b}$$

in which the values of K_S and G may both be considered random variables. In the demonstrations below, one looks at the effective areal relation $f_e(I_e)$ found from combining the parts of (8) as a direct functional equivalent to the point relation [(3)].

Ensemble Effective Infiltration

In the following K_S will be treated as a spatially random variable, having a mean value $\xi_K \equiv \xi(K_S)$ and a coefficient of variation CV_K. The variation of K_S over an area plays a double role in the effective areal value of the infiltration rate. When a rainfall of rate r falls on an area with distributed K_S, there will theoretically be a part of the area that has $K_S > r$, within which the infiltration rate will be r. As first introduced by Hawkins and Cundy (1987) for the steady infiltration case ($f = K_S$), the areal effective value of K_S, which will be called here K_e, can be found from the PDF of K_S, $p_k(K_S)$, and the value of r

$$K_e = [1 - P_k(r)]r + \int_0^r k p_k(k)\, dk \tag{9}$$

Here P_k = CDF of K_S; and the integral term is the "partial" expected value of K_S (the expected value of K_S over the area having $K_S < r$). Hawkins and Cundy (1987) pointed out that (9) can be analytically integrated for the special case of an exponential distribution of K_S. The lognormal distribution function represents measured data much better, for which $p_k(\cdot)$, with mean μ and variance σ^2, may be expressed

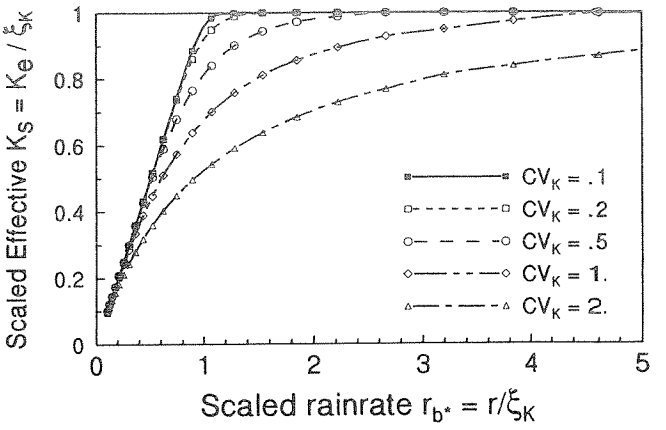

FIG. 3. Effective Value of Ensemble Saturated Conductivity K_e Is Shown for Variety of Values of Coefficient of Variation of K_S (CV_K) for Area of Interest, according to Eq. (10)

$$p_k(x) = \frac{1}{xs\sqrt{2\pi}} \exp\left(\frac{-[\ln(x) - \ln(m)]^2}{2s^2}\right) \tag{10}$$

where $s = \mu(w - 1)^{1/2}$; $m = \mu/w^{1/2}$; and $w = \exp(\sigma^2)$. Chen et al. (1994) used a form of (10) in an expression related to (9), numerically evaluating a complimentary error function. Here (9) is directly numerically integrated for a range of rainfall intensities and relative variabilities, and the data shown in Fig. 3 is obtained. For an area with no variation of K_S, and for $r < K_S$, K_e equals r and no runoff can occur. Also for $CV_K = 0$, K_e is K_S for all rain rates $>K_S$. However, for an area with any significant variation in K_S, the ensemble K_e falls below ξ_K. Because of this, in certain cases runoff can occur for $r < \kappa_K$. For very large intensities, K_e asymptotically approaches ξ_K.

The results presented in Fig. 3 can very accurately be described by a family of empirical curves as follows:

$$\frac{K_e(r_{b^*})}{\xi_K} = \left[1 + \left(\frac{1}{r_{b^*}}\right)^p\right]^{-1/p} \tag{11a}$$

where

$$p = \frac{1.8}{(CV_K)^{0.85}} \tag{11b}$$

where r_{b^*} is defined as r/ξ_K, similar to (2). Thus K_e can easily be evaluated for any CV_K and value of r. The equation holds for values of CV_K even larger than those shown here.

SAMPLING EXPERIMENTS

Distributed K_S

With the numerical LH method one can evaluate $f_e(I_e)$ from the parts of (8) for a distribution of K_S by using a variety of values of r_{b^*} and CV_K. The symbols shown in Figs. 4(a–c) represent the results of simulations for lognormally distributed K_S with a range of values of CV_K and a set of four intensities, with $G\Delta\theta_i = 15$ and $\alpha = 0.85$. The underlying lognormal distribution of K_S was numerically simulated with 30 divisions of the $p_k(\cdot)$ relation. The variation of the ensemble value K_e obtained by sampling simulation, approached asymptotically at large I_e, matches that obtained from (9). In addition, there is no longer a discontinuity in dI_e/dt at a ponding time. Indeed, for a distribution of K_S with limits between 0 and infinity, there is no longer a single ponding time. For a continuously distributed K_S, there would theoretically be some infinitesimal area on which runoff begins almost immediately upon the initiation of rainfall.

The ensemble infiltration curves such as shown in Fig. 4

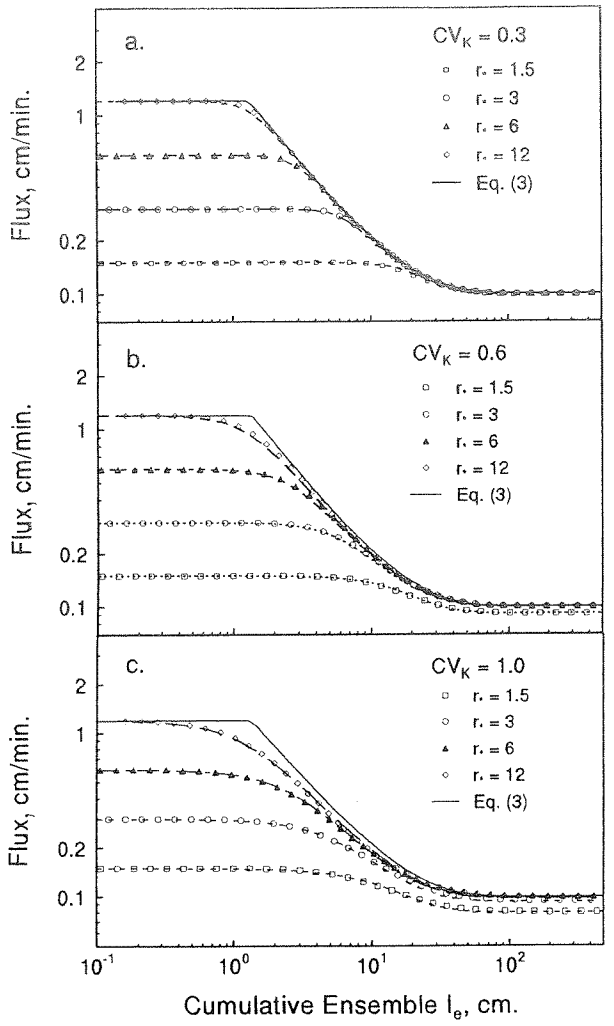

FIG. 4. Areal Effective Infiltration Rate Pattern for Four Values of Scaled Intensity for Different Degrees of Variation of Saturated Hydraulic Conductivity K_S: (a) $CV_K = 0.3$; (b) $CV_K = 0.6$; (c) $CV_K = 1.0$ [Dashed Lines Represent Results for Model of Eqs. (11)–(13)]

can be expressed in terms of the associated values of CV_K and r_*, as was done above to obtain the relation of K_e to r_* [(11)]. Employing scaling transformations as well as the underlying relation of (3), a distributed infiltration expression is formed to describe the results as follows:

$$f_{e^*} = 1 + (r_{e^*} - 1)\left\{1 + \left[\frac{(r_{e^*} - 1)}{\alpha}(e^{\alpha I_{e^*}} - 1)\right]^c\right\}^{-1/c}, \quad r_{e^*} > 1 \tag{12}$$

in which ensemble scaled $r_{e^*} = r/K_e$; ensemble scaled $I_{e^*} = (\int f_e\, dt)/(G\Delta\theta_i)$; and ensemble scaled $f_{e^*} = f_e/K_e$.

A slightly different scaling for r is required in this relationship because of the difference between K_e and ξ_K. Parameter c is to be related to CV_K below.

It is important to note that (12) describes the variation of actual (ensemble) infiltration rate f_e and not the infiltrability f_c, as do point infiltration equations of Smith-Parlange or Green-Ampt [(3), or (4) and (5)]. This means (12) can be used throughout a temporally variable rainfall with changes in r_{e^*} as the storm progresses ($r_{e^*} > 1$), using ensemble I_{e^*} as the continuous independent variable. Ponding time or depth need not be separately calculated (there is no single ponding time). This effectively enables definition of ensemble infiltration rates for changing rainfall rates, illustrated below, and makes it applicable for treating a rainfall rate pattern.

The parameter c in (12) describes the curvature of the ensemble $f_{e^*}(I_*)$ relation in the region of ponding development. As CV_K approaches 0, parameter c becomes large and K_e approaches ξ_K, and as r_{e^*} becomes large (12) approaches the behavior of (3). Simulation of a range of r_{e^*} and CV_K values was used to assess the influence of each of these variables on the ensemble effective relation $f_{e^*}(I_*)$. From these results, for log-normal distribution of K_S, parameter c is related to r_{b^*} and CV_K, as illustrated in Figs. 5 and 6. Fig. 5 shows that at larger values of r_{b^*} the value of c becomes independent of r_{b^*} and only related to CV_K. Reported values of $CV_K > 2$ are unusual [Electrical Power Research Institute (EPPRI) 1985], but the model behaves asymptotically, so extension to $CV_K > 2$ is straightforward. Fig. 6 illustrates this asymptotic relation of c to CV_K. A single empirical equation was developed to describe the relations between c, r_{b^*}, and CV_K in the simulation results

$$c \cong 1 + \frac{0.8}{(CV_K)^{1.3}}[1 - \exp(-0.85(r_{b^*} - 1))] \tag{13}$$

The dashed lines in Figs. 4(a–c) represent the application of (11)–(13) to the ensemble cases numerically simulated. The fit is in all cases quite accurate.

In addition to the change in c due to r and CV_K, there is a slight bias in the effective areal value of G evidenced by the simulation results. This is demonstrated best in Fig. 4(c); note that, in the middle sloping portion of the function, each line falls somewhat below the line of (1). This bias results from the nonlinear nature of the averaging process of (8) in which f_e and I_e are nonlinear functions of K_S. This biasing for log-

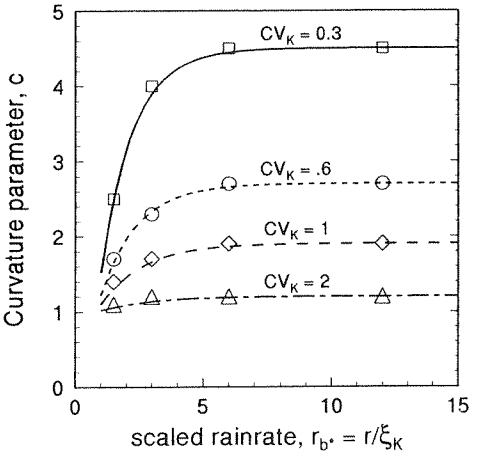

FIG. 5. Systematic Behavior of Parameter c in Eq. (12) as Function of CV_K and Scaled Intensity r_*

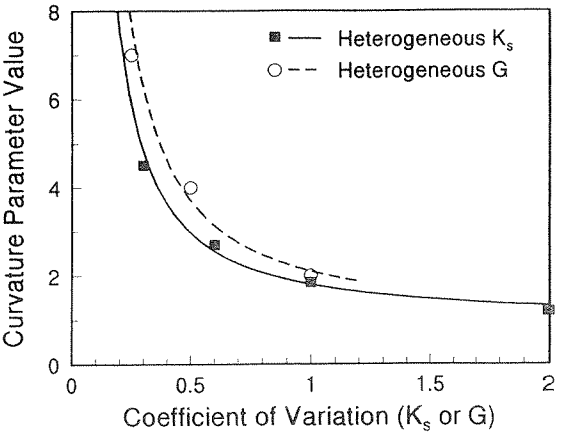

FIG. 6. Variation of c in Response to Various Values of CV_K Is Asymptotically Regular for Large Values of r_* [Eq. (13) Is Shown by Solid Line]

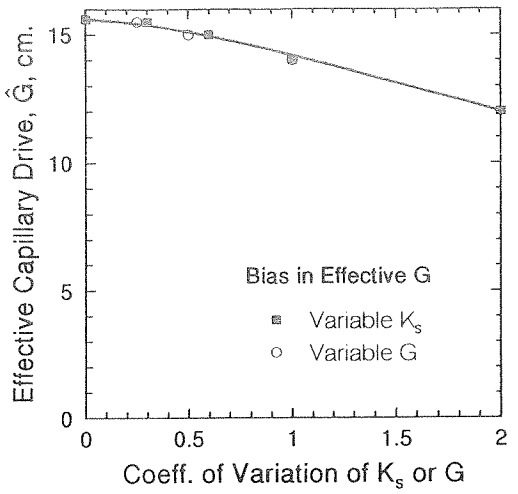

FIG. 7. Bias in Effective Value of $G(G)$ Increases Slightly and Systematically with Increasing CV_K

normal K_S also may be represented using the curve shown in Fig. 7. In this figure spatial effective G is represented by $\hat{G}$.

Distributed G

Variations in capillary parameter G result from variations in a larger number of soil properties than for K_S, including pore-size distribution, soil texture, organic matter, and aggregation. There is much less published data to indicate the relative random variability of G. Smith and Diekkrüger (1992) found G distributed approximately lognormally, with values of the coefficient of variation of G, CV_G, from 0.4 to slightly >1, which are about half the range of variation of K_S.

From (6), it is clear that a distribution of parameter G would have the same effect on f_e at early times (or at small I) as a distribution of K_S. In fact, for infiltration from ponded upper boundary conditions rather than rainfall (where all points on the random K_S surface are producing runoff), there is no distinction in the effects of randomization of the two parameters and they can be considered to act in tandem. For rainfall however, the effects will diverge at larger times, because the function $K_e(r_{b*})$ [(11)] is not dependent on G. The effect of a range of CV_G on $f_e(I_e)$ is illustrated in Fig. 8, which exhibits behavior similar to that which would be expected for variable K_S.

The joint distribution of K_S and G is relevant to simulating ensemble infiltration, and its simulation is straightforward with the LH method. Joint variation would result in additive effects on f_e at early times, to the extent that these two variables were randomly independent. However, in the relative absence of field data for the interrelation of the distribution of these variables, this topic is left for future studies.

Patterns of $r(t)$

The LH simulation of a randomized infiltration surface can be compared with use of the model proposed here to demonstrate that early time variations in r are accurately simulated by application of (11)–(13). For the heterogeneous as well as uniform surfaces, use of $f_e(I_e)$ rather than $f_e(t)$ is important to represent the effect of variations in rainfall intensity on ponding and runoff. An example for a simple case is presented in Fig. 9 for a soil with $CV_K = 1$, and $\alpha = 0.85$. Results are shown in dimensioned form. Rain-rate changes from 0.3 to 0.6 cm/min at 6 min ($I_e = 1.8$ cm) and back to 0.3 cm/min at 25 min. The model simulation is essentially undistinguishable from the ensemble performance. Note that the slight drop in infiltration rate due to reduction in r at 25 min (about $I_e = 7.5$) is reproduced by both model [(12)] and numerical LH sampling simulation.

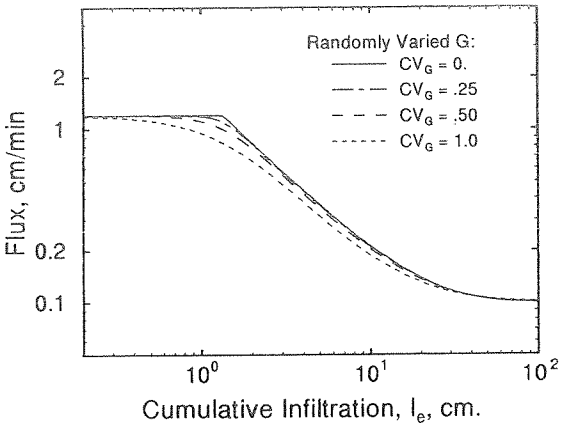

FIG. 8. Variation in G Has Effect on Areal Effective Infiltration Relation $f(I)$ Very Similar to That of Variation in K_S

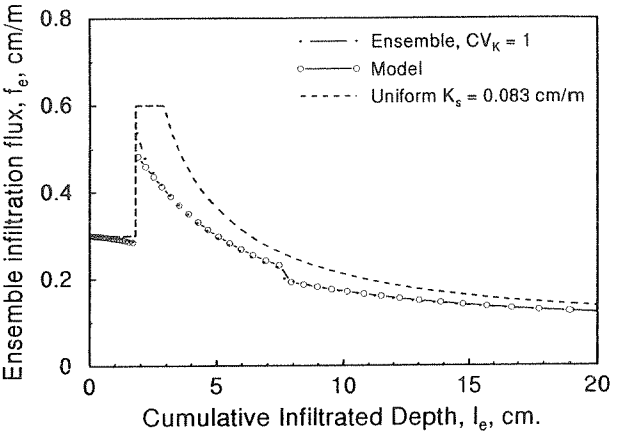

FIG. 9. Using Relation $f(I)$ Rather Than $f(t)$ Allows Simulation of Effect of Changing Value of r Quite Accurately with Eq. (12), as Illustrated Here on Soil with $CV_K = 1$ ($r = 0.3$ cm/m for 6 min and 0.6 cm/min for 19 min) [Open Circles Are Ensemble Simulation with LH Sampling; Results for Use of Eq. (12) Are Shown with Solid Dots]

FIELD EVIDENCE AND MODEL APPLICATION

The two most distinguishing features of the pattern of infiltration from heterogeneous ensembles are the gradual appearance of runoff (no sudden ponding time) and the interaction between effective final infiltration rate and rainfall intensity. Thus for field evidence one looks for these two characteristics in experimental data. Although extensive evidence exists illustrating the highly variable nature of soil hydraulic properties and infiltration [e.g., Nielsen et al. (1973), Bresler and Dagan (1983), Grah et al. (1983), EPRI (1985), and Loague (1986)], there are no carefully designed experimental studies with extensive measurements to determine both the spatial variation of infiltration parameters and the runoff behavior of an area. Such experiments also would require knowledge of the microtopography and organization of rills in relation to the variations in infiltrability due to the interaction of runoff–run-on effects that are likely to interact with the independent sampling that is assumed in the model presented above.

Given the lack of this type of detailed experimental data, one proceeds as follows. First, several modeling studies are discussed in which the results indicate a bias in comparison to observed data that are indicative of heterogenous infiltration impacts on asymptotic infiltration rate. Second, the model presented here will be applied and contrasted to a nonvariable infiltration case and compared to observations that exhibit

some of the characteristics of runoff generated from a heterogeneously infiltrating surface noted above.

The first case is drawn from extensive application of the KINEROS rainfall-runoff-erosion model (Woolhiser et al. 1990) to several of the Lucky Hills subcatchments in the USDA-Agricultural Research Service Walnut Gulch Experimental Watershed, Tombstone, Ariz. (Renard et al. 1993). KINEROS is a distributed kinematic wave model that represents the catchment as a series of cascading overland planes and trapezoidal channels. Within each overland flow plane, infiltration parameters are assumed uniform, and the 1D continuity equation is solved interactively with infiltration [(3)] using finite-difference methods (Woolhiser et al. 1990; Smith et al. 1995). In the application of the model all simulations with uniform K_S assumptions have shown that model predictions are biased higher for larger rainfall intensities (and depths) and relatively lower for small rainfall rates (Goodrich 1990; Goodrich et al. 1993, 1994; Smith et al. 1995). This is the expected behavior of a catchment with small-scale heterogeneity of infiltration rates, as shown above. Fig. 10 illustrates the bias for a set of observed runoff events on Lucky Hills subcatchments 102 (1.4 ha) and 104 (4.4 ha). The value of K_S used for each catchment was found by calibration on one data set and applied to an independent data set (Goodrich 1990). The calibration objective function favors the fit of larger events, and in all cases there was a bias such that small events were almost always underpredicted. This is exactly the expected result for surfaces with small-scale heterogeneities in K_S, based on the results in Fig. 3.

Another study in New Mexico by Gotti (1996) was dramatic in demonstrating the effect of storm size on larger heterogeneous areas. A large number of storm runoff events for a 1 ha catchment were simulated with the KINEROS model [using (3)]. She found that a considerable bias in fitted values of K_S, based on storm size, was necessary to match storm runoff results. To obtain reasonable simulations of measured data, Gotti separated the storms into smaller and larger intensity events and assigned a much smaller value of K_S to the smaller intensity events than to the more intense events. This is again consistent with the expected effects of significant heterogeneity in K_S over the catchment.

A newer version of the KINEROS model [KINEROS2, Smith et al. (1995)] was modified to incorporate the spatially variable infiltration method presented in (12). Examples of application of the model to several cases follows. In the first case the model was applied to the 0.36-ha Lucky Hills 106 subcatchment of Walnut Gulch. The selected event occurred on Aug. 31, 1966, and produced a double-peaked hydrograph with a small amount of runoff occurring in the earliest peak. Parameters for the model were derived strictly from field observations and were not optimized to match the observed hydrograph. Geometric model parameters were derived from a 1:480, 0.3048-m (1-ft) contour interval orthophoto map. The watershed was discretized into 23 overland flow elements contributing to a network of seven channels. The area of each overland flow element as well as a representative flow length was digitized. This length became the length of the overland flow plane. By dividing the area by the flow length, the width of the plane was obtained. During the flow length digitization, the slope of the flow element also was determined using Gray's method (1961). Channel slope and length were obtained in the same manner. Trapezoidal channel geometry for each channel was measured in the field. Hydraulic roughness estimates for each modeling element also were field estimated using guidelines from Engman (1986). Seventeen soil samples were obtained and analyzed to determine their textural properties. From this data, estimates of K_S and G for each sample were obtained from Rawls et al. (1982), with adjustments for rock (>2 mm) using the relationship of Bouwer and Rice (1984). The average K_S from the 17 samples is 13.3 mm/h, with a coefficient of variation CV_K of 0.56. Prestorm estimates of initial soil water content were estimated using the CREAMS water balance model (Knisel 1980). The simulation also was repeated assuming a uniform K_S on each overland flow plane ($CV_K = 0.0$), without altering the mean K_S for each overland flow plane. Results of the simulations are illustrated in Fig. 11. The simulation is clearly improved by incorporating spatial variation of infiltration within the model elements ($CV_K = 0.56$ case).

Two other examples are drawn from rainfall simulator plot studies. The first case uses data from an April 16, 1992, simulator run on a 10.67-m-long by 3.05-m-wide (35 × 10 ft) plot in the Bernardino (thermic *Ustollic Haplargid*) soil complex of the USDA-ARS Walnut Gulch Experimental Watershed (Simanton et al. 1986). The plot contains naturally occurring vegetation cover with 40.9% canopy cover at the time of the simulator run, with a range of surface cover (21.3% rock, 18.2% gravel, 31.5% soil, 18.6% litter, and 10.4% basal vegetation; J. R. Simanton, personal communication, June 26, 1997). Immediately adjacent to the plot and just prior to the simulator run, three ponded disk permeameter measurements were made with a 7-mm head. The average of the steady infiltration rates

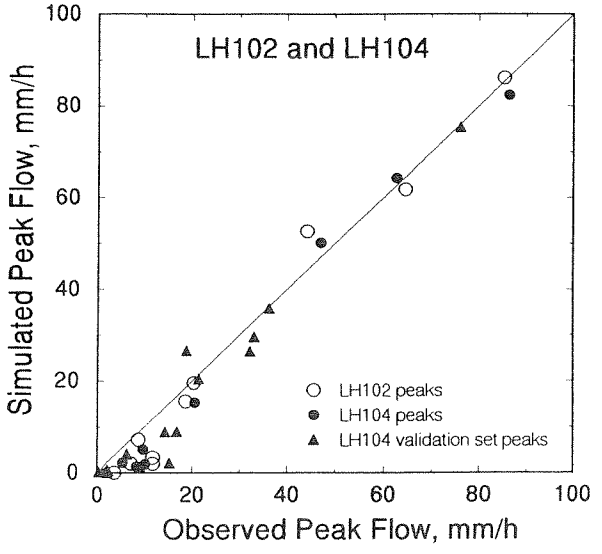

FIG. 10. Analysis of Predictive Capability of Runoff Model with Uniform K_S for Two Small Watersheds in ARS Walnut Gulch, Ariz., Catchment Shows Consistent Underpredicted Flows for Smaller Events as Expected from Results Shown Above for Ensemble Infiltration Simulation

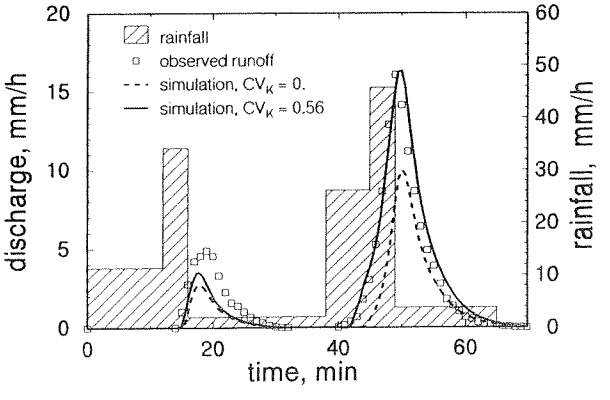

FIG. 11. Inclusion of Spatial Variation in K_S Increases Ability of Dynamic Watershed Simulation Model to Match Measured Data, as Shown Here for Double-Peaked Event on 0.36-ha Lucky Hills, Ariz., Subcatchment (Mean K_S Values Are Unchanged between $CV_K = 0.56$ and 0.0 Simulations)

for three measurements was 128.4 mm/h with a coefficient of variation of 0.37. A rotating boom rainfall simulator (Weltz et al. 1992) was then used to apply rainfall with a nearly constant intensity of 61 mm/h for 23 min. KINEROS2 was run for this plot, and rainfall input using K_S and CV_K was derived from the disk permeameter measurements. Measured and simulated results are illustrated in Fig. 12. Note that using the CV_K derived from the three disk measurements produces a simulated runoff hydrograph that grossly underestimates the observed data. However it should be noted that the disk permeameter [20.2-cm (8-in.) diameter] requires a bare soil area without rock cover for the measurements. Given the variability of both surface and canopy cover in the larger simulator plot, it is reasonable to assume the CV_K would be larger than obtained from the three disk measurements. When the KINEROS2 simulation is repeated with CV_K increased to 1.0, the resulting simulated hydrograph closely resembles the observations. Simulation using the average of the disk data for K_S (CV_K = 0.0) produces no runoff. Admittedly, CV_K was selected based on the observations, but it falls well within realistic values based on field observations (Nielsen et al. 1973; EPRI 1985).

A second case involves plot data on a heavier, fine-textured loam soil at Chickasaw, Okla. The plot has a 5% slope and a 62% cover of grazed grass, with a Manning's n of 0.54 estimated by Weltz et al. (1992). Experiments were done with the same equipment as for the previous plot. Simulations with K_S = 3 mm/h do not match the later part of the runoff, and simulations with K_S = 4 mm/h do not start at the right time. Including a distribution of K_S with CV_K = 1.0, however, improves the simulation in both regions, as illustrated in Fig. 13.

Several items are worth noting in the above examples. There is a compensating interaction between the mean K_S and CV_K for overall runoff volume production (excess rainfall). A lower mean K_S will produce more runoff, as will increasing the spatial variability of infiltration via increasing CV_K. However, the dynamic behavior of the simulated hydrograph cannot be easily matched by altering one or other of the parameters. In the Lucky Hills 106 simulation example in Fig. 11, if K_S is decreased to match the second peak and CV_K is set to zero, the first peak is overestimated. This is further illustrated in the simulator plot example of Fig. 13. In this case the peak rate can be matched by decreasing K_S, but both the initial start-up of runoff and peak cannot be simulated without incorporation of infiltration variability. The point that an additional parameter or degree of freedom is added to the model to enhance

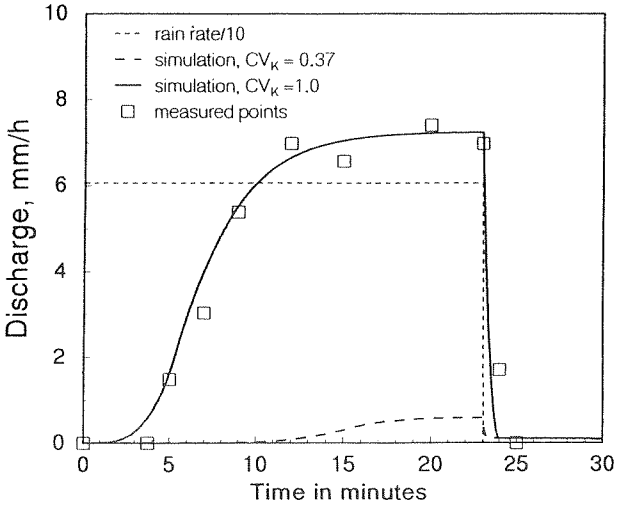

FIG. 12. Walnut Gulch Plot Runoff Shown Here Is Only Simulated when Infiltration Model Includes Effect of Significant Heterogeneity in K_S (Using Plot Average Value of Three Measurements of K_S Produces No Runoff)

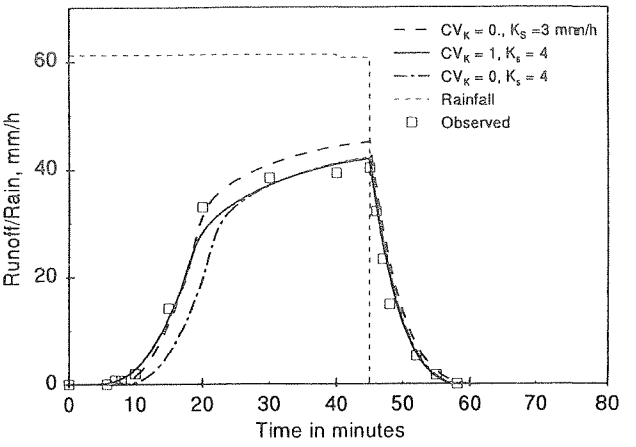

FIG. 13. This Plot Runoff Simulation for Experiment on Loam Soil near Chickashaw, Okla., Demonstrates Additional Improvement in Accuracy Afforded by Inclusion of Distribution of K_S, Obtaining Simulation Accuracy that Could Not Be Achieved by Adjusting Mean Value of K_S Alone

model fitting capability also should be noted. Although the addition of a parameter does inherently increase the fitting degrees of freedom, it should not be expected that spatial heterogeneity could be treated without any additional parameters. The model developed to treat infiltration variability extends a physically based, parsimonious function. It adds only one additional parameter and is numerically efficient. The examples above, albeit with limited measurements of heterogeneity, illustrate the ability to more realistically simulate observations of runoff generation on heterogeneous watersheds or hillslopes. Further physical model discretization of a hillslope or watershed to treat small-scale infiltration variation is impractical and for each new model element would add a full suite of both hydraulic and infiltration model parameters, whereas the model presented herein accomplishes this with a single additional parameter.

SUMMARY AND CONCLUSIONS

Large, extreme runoff events are dominated by rainfall, and infiltration plays a smaller role in such cases. However, as demonstrated here and in previous studies, the inclusion of infiltraton heterogeneity is valuable for treating the total range of runoff events representing the general water resources picture of a catchment. Developed and demonstrated here is a model for field-scale infiltration, which can reflect the degree of random variation of infiltration parameters over an area. Unlike previous such models, (12) does not require extensive numerical or Monte-Carlo procedures to represent heterogeneity, making it more suitable for hydrologic practice. The random variation of either of the two basic infiltration parameters can be easily represented by a single additional parameter. The model is presented in normalized form and is applicable to infiltration/runoff for any soil and any pattern of rainfall.

Field measurements from both plots and small watersheds suggest that inclusion of the effect of distributed K_S in simulations using this model can significantly improve runoff estimation. Application of the model described here improves the accuracy of simulation over a range of storms and catchment sizes.

ACKNOWLEDGMENTS

Special thanks are extended to Roger Simanton for providing and interpreting the rainfall simulator data, to Rose Shillito for providing the disk permeameter data, and to Carl Unkrich for assistance in programming and carrying out a number of the computer simulations.

APPENDIX. REFERENCES

Bouwer, H., and Rice, R. C. (1984). "Hydraulic properties of stony vadose zones." *Ground Water*, 22(6), 696–705.

Bresler, E., and Dagan, G. (1983). "Unsaturated flow in spatially variable fields 2. Application of water flow models to various fields." *Water Resour. Res.*, 19(2), 421–428.

Chen, Z., Govindaraju, R. S., and Kavvas, M. L. (1994). "Spatial averaging of unsaturated flow equations under infiltration conditions over areally heterogeneous fields 2. Numerical simulations." *Water Resour. Res.*, 30(2), 535–548.

Electrical Power Research Institute (EPRI). (1985). "Spatial variability of soil physical properties in solute migration: A critical literature review." *Rep. EA-4428, Prepared by Univ. of Calif. at Riverside for EPRI*, Palo Alto, Calif.

Engman, E. T. (1986). "Roughness coefficients for routing surface runoff." *J. Irrig. and Drain. Engrg.*, ASCE, 112(1), 39–53.

Goodrich, D. C. (1990). "Geometric simplification of a distributed rainfall-runoff model over a range of basin scales." PhD dissertation, Dept. of Hydro. and Water Resour., University of Arizona, Tucson, Ariz.

Goodrich, D. C., et al. (1994). "Runoff simulation sensitivity to remotely sensed initial soil water content." *Water Resour. Res.*, 30(5), 1393–1405.

Goodrich, D. C., Stone, J. J., and Van der Zweep, R. (1993). "Validation strategies based on model application objectives." *Proc., Fed. Interagency Workshop of Hydrologic Modeling Demands for the 90's, USGS Water Resour. Investigations Rep. 93-4018*, USGS, Reston, Va., 8-1–8-8.

Goodrich, D. C., Woolhiser, D. A., and Sorooshian, S. (1988). "Model complexity required to maintain hydrologic response." *Proc., 1988 Nat. Conf., Hydr. Engrg.*, ASCE, New York, 431–436.

Gotti, N. L. (1996). "Testing a physically-based distributed model (KINEROS): Predicting runoff and erosion from a semi-arid hillslope in the southwestern United States." MS thesis, Dept. of Civ. and Envir. Engrg., Massachusetts Institute of Technology, Cambridge, Mass.

Grah, O. J., Hawkins, R. H., and Cundy, T. W. (1983). "Distribution of infiltration on a small watershed." *Proc., ASCE Specialty Conf. on Advances in Irrigation and Drainage*, J. Dorelli, et al., eds., ASIE, New York, 44–54.

Gray, D. M. (1961). "Synthetic unit hydrographs for small watersheds." *J. Hydr. Div.*, ASCE, 87(4), 33–54.

Grayson, R. B., Moore, I. D., and McMahan, T. A. (1992). "Physically-based hydrologic modeling, 2, Is the concept realistic?" *Water Resour. Res.*, 28(10), 2659–2666.

Green, W. H., and Ampt, G. (1911). "Studies of soil physics, Part I. The flow of air and water through soils." *J. Agric. Sci.*, 4, 1–24.

Hawkins, R. H., and Cundy, T. W. (1987). "Steady-state analysis of infiltration and overland flow for spatially-varied hillslopes." *Water Resour. Bull.*, 32(2), 251–256.

Hjelmfelt, A. T., and Burwell, R. E. (1984). "Spatial variability of runoff." *J. Irrig. and Drain. Engrg.*, ASCE, 110(1), 46–54.

Knisel, W. G., ed. (1980). "CREAMS: A field scale model for chemicals, runoff, and erosion from agricultural management systems." *Conservation Res. Rep. 26*, Sci. and Educ. Admin., U.S. Department of Agriculture, Washington, D.C.

Loague, K. M. (1986). "An assessment of rainfall-runoff modeling methodology." PhD dissertation, University of British Columbia, Vancouver, 140–161.

McKay, M. D., Beckman, R. J., and Connover, W. J. (1979). "A comparison of three methods for selecting values of input variables in the analysis of output from a computer code." *Technometrics*, 21(2), 239–245.

Maller, R. A., and Sharma, M. L. (1981). "An analysis of areal infiltration considering spatial variability." *J. Hydro.*, Amsterdam, 52, 25–37.

Nachabe, M. H., Illangasekare, T. H., Morel-Seytoux, H. J., Ahuja, L. R., and Ruan, H. (1997). "Infiltration over heterogenous watershed: Influence of rain excess." *J. Hydrologic Engrg.*, ASCE, 2(3), 140–143.

Nielsen, D. R., Biggar, J. W., and Erh, K. T. (1973). "Spatial variability of field measured soil-water properties." *Hilgardia*, 42, 215–259.

Parlange, J.-Y., Lisle, I., Braddock, R. D., and Smith, R. E. (1982). "The three-parameter infiltration equation." *Soil Sci.*, 133(6), 337–341.

Philip, J. R. (1957). "The theory of infiltration, 4. Sorptivity and algebraic infiltration equations." *Soil Sci.*, 84, 257–264.

Philip, J. R. (1985). "Reply to 'Comments on steady infiltration from spherical cavities.'" *Soil Sci. Soc. Am. J.*, 49(3), 788–789.

Rawls, W. J., Brakensiek, D. L., and Saxton, K. E. (1982). "Estimation of soil water properties." *Trans. ASAE*, 25 SW, 1316–1320, 1328.

Renard, K. G., et al. (1993). "Agricultural impacts in an arid environment: Walnut Gulch case study." *Hydrological Sci. and Technol.*, 9(1–4), 145–190.

Sharma, M. L., Gander, G. A., and Hunt, C. G. (1980). "Spatial variability of infiltration in a watershed." *J. Hydro.*, Amsterdam, 45, 101–122.

Simanton, J. R., Johnson, C. W., Nyhan, J. W., and Romney, E. M. (1986). *Proc., Rainfall Simulator Workshop, Rainfall Simulation on Rangeland Erosion Plots*, Society Range Management, Denver, 11–17.

Sivapalan, M., and Wood, E. F. (1986). "Spatial heterogeneity and scale in the infiltration response of catchments." Chapter 5, *Scale problems in hydrology*, V. K. Gupta, I. Rodriguez-Iturbe, E. F. Wood, eds., Reidel, Hingham, Mass., 81–106.

Smith, R. E., Corradini, C., and Melone, F. (1993). "Modeling infiltration for multistorm runoff events." *Water Resour. Res.*, 29(1), 133–144.

Smith, R. E., and Diekkrüger, B. (1992). "Field-scale soil water flow in heterogeneous soils I. Modeling statistical soil variation and large-scale constituent relations." *Modeling Geo-Biosphere Processes*, 1, 205–227.

Smith, R. E., Goodrich, D. C., and Woolhiser, D. A. (1990). "Areal effective infiltration dynamics for runoff on small catchments." *Proc., Trans. 14th Int. Congr. of Soil Sci.*, Vol. I, International Society of Soil Science, Wageningen, The Netherlands, Commission I, 22–27.

Smith, R. E., Goodrich, D. C., Woolhiser, D. A., and Unkrich, C. L. (1995). "KINEROS—A KINEmatic Runoff and EROSion Model." Chapter 20, *Computer models of watershed hydrology*, V. P. Singh, ed., Water Resources Publications, Highlands Ranch, Colo., 697–732.

Smith, R. E., and Hebbert, R. H. B. (1979). "A Monte Carlo analysis of the hydrologic effects of spatial variability of infiltration." *Water Resour. Res.*, 15(2), 419–429.

Smith, R. E., and Parlange, J.-Y. (1978). "A parameter-efficient hydrologic infiltration model." *Water Resour. Res.*, 14(3), 533–538.

Vieira, S. R., Nielsen, D. R., and Biggar, J. W. (1981). "Spatial variability of field-measured infiltration rate." *Soil Sci. Soc. Am. J.*, 45(6), 1040–1048.

Weltz, M. A., Arslan, A. B., and Lane, L. J. (1992). "Hydraulic roughness coefficients for native rangelands." *J. Irrig. and Drain. Engrg.*, ASCE, 118(5), 776–790.

White, I., and Sully, M. J. (1987). "Macroscopic and microscopic capillary length and time scales from field infiltration." *Water Resour. Res.*, 23(8), 1514–1522.

Woolhiser, D. A., and Goodrich, D. C. (1988). "Effect of storm rainfall intensity patterns on surface runoff." *J. Hydro.*, Amsterdam, 102, 335–354.

Woolhiser, D. A., Goodrich, D. C., Emmerich, W. E., and Keefer, T. O. (1990). "Hydrologic effects of brush to grass conversion." *Proc., ASCE IR Div. Symp., Watershed Plng. and Anal. in Action*, ASCE, New York, 293–302.

Woolhiser, D. A., Smith, R. E., and Giraldez, J-V. (1996). "Effects of spatial variability of saturated hydraulic conductivity on Hortonian overland flow." *Water Resour. Res.*, 32(3), 671–678.

Yeh, T.-C. J., Gelhar, L. W., and Gutjahr, A. L. (1985). "Stochastic analysis of unsaturated flow in heterogeneous soils, 1. Statistically isotropic media." *Water Resour. Res.*, 21(4), 447–456.